Chaotic Scattering and Self-Organization in Spheromak Sustainment

John M. Finn and Carl R. Sovinec
Theoretical Division, Los Alamos National Laboratory, Los Alamos, New Mexico 87545

Diego del-Castillo-Negrete
Oak Ridge National Laboratory, Oak Ridge, Tennessee 37831
(Received 7 June 2000)

Flux core spheromak sustainment by electrostatic helicity injection is studied in resistive MHD. The geometry has magnetized electrodes at the ends held at a potential difference V. For $V > V_c$ the central current column is kink unstable. The nonlinear state with V just above V_c has a large volume of flux surfaces, with rotational transform provided by the helical kinking of the column. As V increases the kink becomes stronger, the tori are destroyed, and the field lines exhibit chaotic scattering. The distribution of field line lengths L, related to confinement and parallel current density, is studied. At larger V or larger Lundquist number S, a limit cycle appears.

PACS numbers: 52.65.Kj, 05.45.-a, 52.55.Hc

Electrostatic helicity injection is a method which has been successful in forming and sustaining spheromak configurations [1–5]. In this scheme, current is driven across two electrodes linked by magnetic flux. The most commonly used design is that of the coaxial gun spheromak, in which the electrodes form a magnetized Marshall gun [1,2]. A related design is that of the flux core spheromak, in which the electrodes are at opposite ends of the device [6–9]. In this Letter we study spheromak formation and sustainment in the latter case and idealize the geometry as a cylinder of finite length with magnetic flux through the end caps, which are held at a fixed potential V.

In spheromak sustainment, three dimensional (3D) processes must occur: by the Cowling theorem [10,11] an axisymmetric spheromaklike state with a volume of nested flux surfaces cannot be maintained against resistive decay. Therefore spontaneous nonaxisymmetric processes in the plasma must play a crucial role in the sustainment process. This Letter describes the first detailed computations of dynamo activity in electrostatically driven spheromaks.

We model the plasma by resistive magnetohydrodynamics (MHD) in three dimensions with finite viscosity and zero β. Specifically, the equations integrated are

$$\rho(\partial_t \vec{v} + \vec{v} \cdot \nabla \vec{v}) = \vec{j} \times \vec{B} + \mu \nabla^2 \vec{v}\,, \qquad (1)$$

$$\vec{E} + \vec{v} \times \vec{B} = \eta \vec{j} \qquad (2)$$

plus Faraday's law. These equations are integrated using the NIMROD code [12]. The profile of the magnetic field in the perfectly conducting electrode surfaces takes two forms, either uniform field or a field distributed according to the 1D paramagnetic pinch profile [13] for the potential V. (The boundary conditions are Dirichlet on $\vec{v}$ and on the normal component $\vec{B} \cdot \vec{n}$, Neumann on $\vec{n} \times \vec{B}$.) The uniform density is not evolved: Its magnitude determines the Lundquist number, but its profile does not play an important role for $\beta = 0$. The dimensionless parameters are (i) H/R, the cylinder height relative to the radius, (ii) the Lundquist number S, the ratio of the resistive time τ_r to the Alfvén time, and (iii) $V_a = \tau_r V/\Psi_e$, the potential scaled to the electrode flux Ψ_e and τ_r. The resistivity and kinematic viscosity are equal. The results show no qualitative differences between the two models for electrode flux distribution. These effects and those of varying the dissipation coefficients, as well as convergence with respect to grid and time step, are discussed in Ref. [14].

For low V_a, the time asymptotic state is a 2D paramagnetic pinch, i.e., an axisymmetric Ohmic equilibrium. All field lines in this 2D paramagnetic pinch state connect the electrodes, and there are no closed flux surfaces, in agreement with the Cowling theorem.

For $S = 1000$, $H/R = 1$, the paramagnetic pinch profile is found to be kink unstable (in the presence of resistivity) for $V_a > 28$. This value corresponds to a twist in the field lines between electrodes $\Delta\theta = 3.3$ near the z axis and $\Delta\theta = 6.0$ for $r/R = 1/3$. The unstable mode is similar to kinks in RFP (reversed field pinch) and tokamak geometry, except that the threshold V_a, which depends strongly on H/R, is influenced by line tying [15,16]. The observed nonlinear time asymptotic state is a steady state kinked pinch. A Poincaré surface of section of the field lines for a case with $V_a = 31$, $S = 1000$, $H/R = 1$ and with flux distributed according to the paramagnetic pinch is shown in Fig. 1. Figure 1 shows a large area of field lines lying on invariant tori or flux surfaces. In this and typical cases for V_a just above the kink instability threshold, there is no separatrix separating these field lines from those directly connecting the electrodes. Rather, there is a small class of chaotic field lines connecting the electrodes. Because these field lines intersect the electrodes, the dynamics is described by *chaotic scattering* [17]. The length L of the field lines connecting the electrodes, similar to the time delay function of chaotic scattering, is shown in Fig. 2. For $x < -0.5$, $x > 0.4$ structures similar to the fractals associated with chaotic scattering are observed. However, this behavior is in a region where B_z

 0031-9007/00/85(21)/4538(4)$15.00 © 2000 The American Physical Society

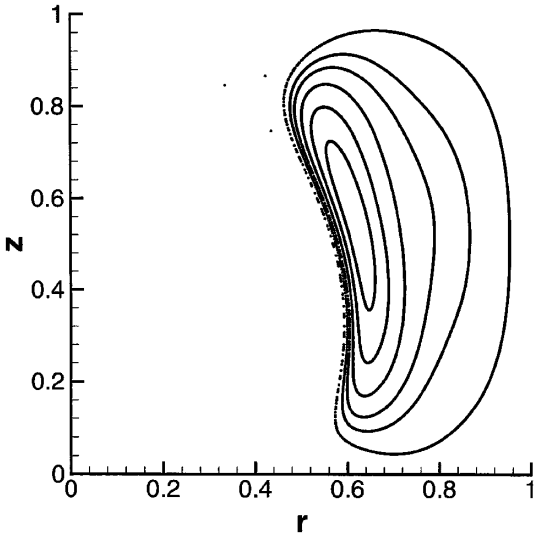

FIG. 1. Poincaré surface of section $\phi = 0$ for the weakly driven case, with $V_a = 31$, $S = 1000$, $H/R = 1$, and with distributed electrode flux. Field lines encircled by the flux surfaces exit rapidly; the three points near $r = 0.45$, $z = 0.8$ exit after one intersection.

on the electrode is very small, so that the fraction of field lines exhibiting chaotic scattering, measured by the flux, is very small. Because of the existence of flux surfaces, the dynamics has characteristics of *nonhyperbolic* chaotic scattering [17,18]: The field line lengths have evidence of the "castlelike" structure seen in Ref. [19].

These steady state solutions are 3D Ohmic equilibria which have a large region of good flux surfaces. In this sense they are similar to the helically symmetric Ohmic equilibria which can exist in RFP geometry [11]. However, since the flux surfaces are not connected to the electrodes, there is no net current driven on them: Consider the flux surface average of the parallel projection of Eq. (2) for time independent fields,

$$\langle \eta \lambda B^2 \rangle = -\langle \vec{B} \cdot \nabla \Phi \rangle = 0 , \tag{3}$$

where Φ is the electrostatic potential, $\langle \cdots \rangle$ is the flux surface average, and $\lambda = \vec{j} \cdot \vec{B}/B^2$. A similar relation has been derived based on magnetic helicity arguments [20]. Perpendicular forces due to viscous and inertial terms are present, although relatively small, and the closed flux surfaces therefore have small perpendicular currents $\vec{j}_\perp$ balancing these forces. The Pfirsch-Schlüter current described by λ and associated with $\vec{j}_\perp$ averages to zero in the sense of Eq. (3). On each open field line, similar field line integration leads to

$$V = \int \eta \lambda B^2 dl/B = L \langle \eta \lambda B \rangle_{fl} , \tag{4}$$

where the integral is between the footpoints on the two electrodes, L is the field line length, and $\langle \cdots \rangle_{fl}$ is the field line average. Since the resistivity η is constant except very near the wall, Eq. (4) indicates that the field line average of the parallel current density λB scales as $1/L$. Most of the field lines connect directly to the electrodes without encircling the flux surfaces (tori), so that $L \sim H$. However, for the few long field lines which encircle the region of tori several times, L is large and $\langle \lambda B \rangle_{fl}$ is small. Typical values of λ for field lines connected to the electrodes are indeed observed to be many times larger than those in the closed flux surface region. If the perpendicular forces (viscous and inertial) in Eq. (1) are negligible, then the current density is force free, i.e., $\vec{j} = \lambda \vec{B}$, and λ is constant on the field lines. In this case Eq. (3) reduces to $\lambda = 0$ in the region of good flux surfaces (and on the magnetic axis). Similarly, if $\vec{j}_\perp = 0$ on the open field lines, Eq. (4) gives $V = \lambda L \langle \eta B \rangle_{fl}$.

A region of closed flux surfaces with a magnetic axis (an elliptic closed field line) as described above can exist with zero average current density (zero current density if $\vec{j}_\perp = 0$) because the fields are nonaxisymmetric. The rotational transform on the flux surfaces is caused by the helical nature of the current density in the central column rather than in stellarator windings [21].

We have computed the safety factor q for the actual fields of Fig. 1 and for the $n = 0$ part of the fields. The actual q is of order 10 and larger than that computed from the $n = 0$ fields by about a factor of 2. That is, there is very little poloidal flux on closed surfaces in this case, and the axisymmetric fields in fact overestimate this flux.

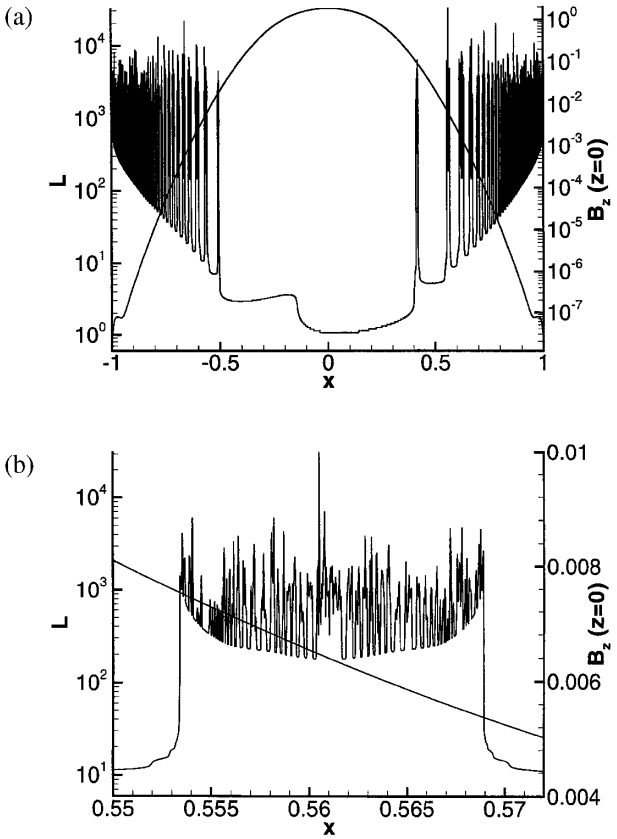

FIG. 2. Field line length L (a) as a function of x on the bottom electrode at $y = 0$, with B_z along the same curve, for the case of Fig. 1; (b) expansion of the scale around $x = 0.56$.

As V_a is increased, the amplitude of the kink increases. Poincaré surfaces of section for such cases show that the flux surfaces begin to disappear as this happens. We show in Fig. 3 the contours of the $n = 0$ component of $\psi = rA_\theta$ for a case with $V_a = 150$, $S = 5000$, $H/R = 1.5$, and with uniform field through the electrodes. The flux amplification, defined as Ψ_a/Ψ_e, where Ψ_a is the $n = 0$ poloidal flux in excess of Ψ_e, is 257%. In contrast, the flux amplification factor for the case of Figs. 1 and 2 is 3%. There is a large class of short field lines that connect fairly directly to the electrodes, and other longer field lines. The length L can again be described by chaotic scattering. The map of the field lines from the bottom surface $z = 0$ to $z = H/2$ and to $z = H$ is shown in Fig. 4 for the case of Fig. 3. Because B_z is uniform for this case, the initial points are picked randomly on $z = 0$ and coded by initial radius. The intersections with $z = H/2$ have empty regions showing the presence of a very small region of tori and the curve $B_z = 0$ ($r \approx 0.7$). The apparent fractal nature of the map, with regions separated by the stable manifolds of the chaotic set, is evident [21]. A plot of L as a function of position on $z = 0$ is shown in Fig. 5. Regions of smooth behavior where L has minima, separated by the (fractal) stable manifold of the chaotic set, where $L \to \infty$, are seen. In Fig. 6 we show the distribution function $f(L)$ for this case. There are several peaks in Fig. 6 most evident for short values $L < 50$. These peaks are traced to the relative minima of L in regions separated by the stable manifold. There is also evidence of an exponential tail for $30 < L < 200$. There is a tail for larger L, but it is not possible to conclude that it obeys a power law [22]; this is consistent with the smallness of the region of closed flux surfaces in Fig. 4. As shown in Fig. 6, there is a fairly large number of long field lines $L \gg H$, which may provide some thermal insulation from the electrode surfaces. However, as discussed above, these long field lines have the lowest value of current density $\langle \lambda B \rangle_{fl}$ and, therefore, the lowest Ohmic heating and are intermittently mixed with the short field lines.

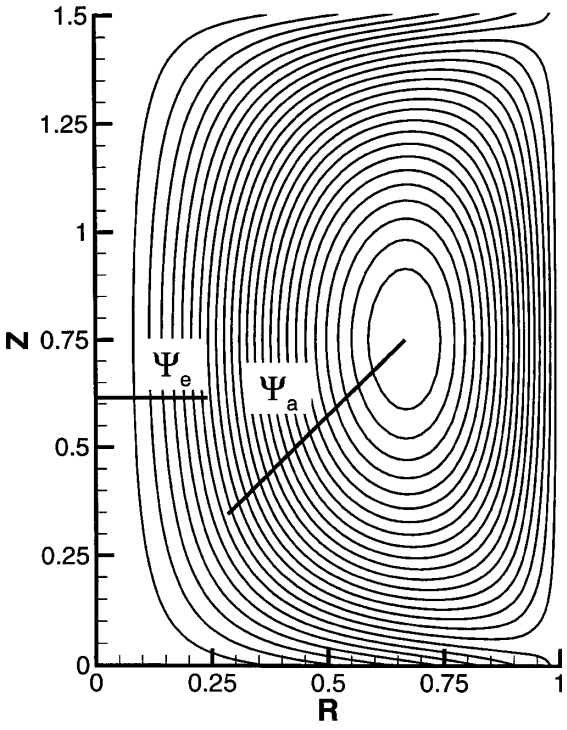

FIG. 3. Contours of axisymmetric ($n = 0$) poloidal flux for a strongly driven case with $V_a = 150$, $S = 5000$, $H/R = 1.5$ and with uniform magnetic field through the electrodes; Ψ_e and Ψ_a are, respectively, the electrode flux and the amplified flux in excess of Ψ_e.

For higher V_a or for higher S a periodic limit cycle appears. There are two distinct parts to the cycle, leading to a sawtoothlike nature. For limit cycle cases, there are few or no invariant flux surfaces.

The spheromak concept is appealing and potentially useful because the magnetic configuration is spontaneously created by the plasma dynamics. The 3D MHD activity creates new structures which break the axisymmetry of the externally applied fields; in this sense a spheromak is a self-organized confinement device. In the low V cases the spontaneously formed structure or pattern is the toroidal region of good flux surfaces. For the strongly driven cases, the self-organized structure is related to the chaotic scattering of the open field lines. In an RFP, on the other hand, the field lines are thought to be chaotic [23] but have a bounding flux surface at the wall. In such cases, essentially all field lines are equivalent. In chaotic scattering this is far from the case, as illustrated by the distribution $f(L)$ in Fig. 6.

These self-organized structures need to be optimized with regard to confinement and heating. The weakly driven cases with good flux surfaces have the possibility of confinement, but there is no Ohmic heating by net current density in the closed flux surface region. Furthermore,

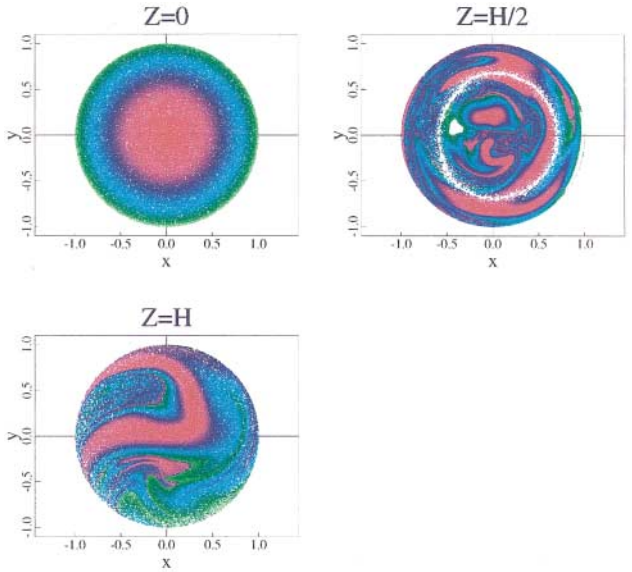

FIG. 4 (color). Map of field lines for the case of Fig. 3 from the bottom to $z = H/2$ and to $z = H$.

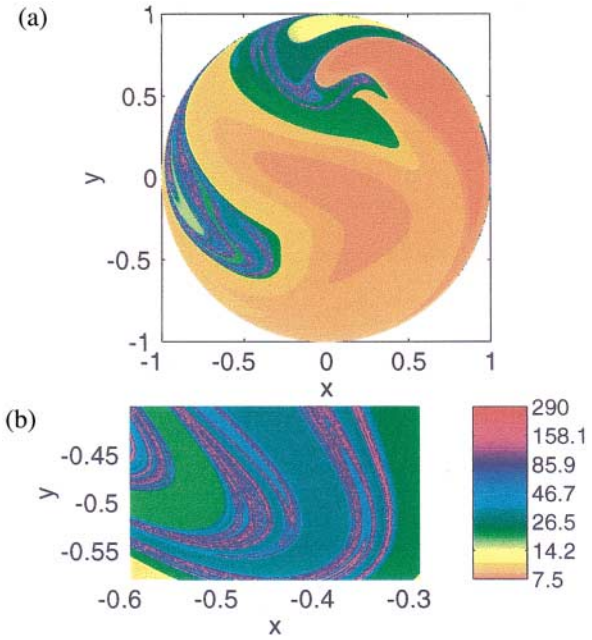

FIG. 5 (color). Field line length as a function of position (a) on lower electrode for the case of Fig. 4; (b) blowup of scale around $x = -0.5$, $y = -0.5$.

the safety factor q is typically very large, and, therefore, effects related to variation of $|\vec{B}|$ on flux surfaces, e.g., neoclassical transport, are very large. It is possible that further optimization to increase the amount of poloidal flux is possible. For example, the distribution of the flux through the electrodes or the electrode geometry could be varied. Bootstrap current should help in this regard, and heating could be provided by rf.

The strongly driven cases have no appreciable volume of flux surfaces, and the longest field lines have the smallest average current density and thus weak Ohmic heating. It is possible that with moderate driving there are small areas of flux surfaces, with the field lines coming near these areas being long enough to give some confinement along field lines. For such cases, the confinement may be similar to typical RFPs, in which the chaos can be characterized by a relatively small field line diffusivity. The strongly driven cases are the most similar to spheromak experiments to date, which have flux amplification factors of several hundred percent. Based on the relatively good confinement of decaying spheromaks [24] and simulations showing the existence of a volume of magnetic surfaces for decaying cases [25] it may be possible to optimize in this range by pulsing the applied voltage V periodically in time.

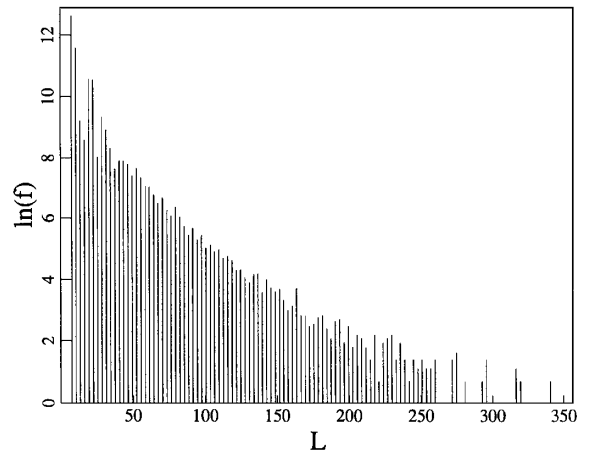

FIG. 6. Distribution $f(L)$ of field line lengths for the case of Fig. 4.

We thank the NIMROD team for development of the numerical methods and code. This work was supported by the U.S. Department of Energy.

[1] W. C. Turner, G. C. Goldenbaum, E. H. A. Granneman, J. H. Hammer, C. W. Hartman, D. S. Prono, and J. Taska, Phys. Fluids **26**, 1965 (1983).
[2] T. R. Jarboe, I. Henins, A. R. Sherwood, C. W. Barnes, and H. W. Hoida, Phys. Rev. Lett. **51**, 39 (1983).
[3] T. R. Jarboe, Plasma Phys. Controlled Fusion **36**, 945 (1994).
[4] E. B. Hooper, J. H. Hammer, C. W. Barnes, J. C. Fernández, and F. J. Wysocki, Fusion Technol. **29**, 191 (1996).
[5] M. G. Rudbridge, S. J. Gee, P. K. Browning, G. Cunningham, R. C. Duck, A. al-Karkhy, R. Martin, and J. W. Bradley, Plasma Phys. Controlled Fusion **39**, 683 (1997).
[6] T. H. Jensen and M. S. Chu, J. Plasma Phys. **25**, 459 (1981).
[7] J. B. Taylor and M. F. Turner, Nucl. Fusion **29**, 219 (1989).
[8] J. M. Finn and P. N. Guzdar, Phys. Fluids B **3**, 1041 (1991).
[9] M. Katsurai, Fusion Technol. **27**, 97 (1995).
[10] T. G. Cowling, Mon. Not. R. Astron. Soc. **94**, 39 (1934).
[11] J. M. Finn, R. Nebel, and C. Bathke, Phys. Fluids B **4**, 1262 (1992).
[12] A. H. Glasser, C. R. Sovinec, R. A. Nebel, T. A. Gianakon, S. J. Plimpton, M. S. Chu, D. D. Schnack, and the NIMROD Team, Plasma Phys. Controlled Fusion **41**, A747 (1999).
[13] R. J. Bickerton, Proc. R. Soc. London **72**, 618 (1958).
[14] C. R. Sovinec, J. M. Finn, and D. del-Castillo-Negrete, "Formation and Sustainment of Spheromaks in the Resistive MHD Model" (to be published).
[15] A. W. Hood and E. R. Priest, Solar Phys. **64**, 303 (1979).
[16] M. Velli, G. Einaudi, and A. W. Hood, Astrophys. J. **350**, 428 (1990).
[17] E. Ott, *Chaos in Dynamical Systems* (Cambridge University Press, Cambridge, England, 1993), pp. 166–176, and references therein.
[18] Y. T. Lau, J. M. Finn, and E. Ott, Phys. Rev. Lett. **66**, 978 (1991).
[19] Y. T. Lau and J. M. Finn, Astrophys. J. **366**, 577 (1991).
[20] A. Boozer, Phys. Fluids B **5**, 2271 (1993); R. Moses, R. Gerwin, and K. Schoenberg, "Current Drive by Magnetic Helicity Injection" (to be published).
[21] Y. T. Lau and J. M. Finn, Phys. Plasmas **3**, 3983 (1996).
[22] C. F. F. Karney, Physica (Amsterdam) **8D**, 360 (1983).
[23] D. D. Schnack, E. J. Caramana, and R. A. Nebel, Phys. Fluids **28**, 321 (1984).
[24] T. R. Jarboe, F. J. Wysocki, J. C. Fernández, I. Henins, and G. J. Marklin, Phys. Fluids B **2**, 1342 (1990).
[25] C. R. Sovinec, Bull. Am. Phys. Soc. **41**, 416 (1999).